Onset of the monsoon in the Miocene drove an increase in chemical weathering in the Ganges-Brahmaprutra watersheds, resulting in a shift from mechanical weathering (tektosilicates, plus mica, illite, and chlorite) to chemical weathering (secondary detrital PCM; smectite, kaolinite) (*36*). The later PCM mineral assemblage resulted in an ~fourfold increase in organic loading and substantially increased the organic carbon burial flux (*36*).

The global change that promoted the rise of animals by 0.6 Ga (*37*) remains one of the most important yet least understood events in the geobiologic record. Here we adopt a non-uniformitarian approach by identifying an important component of the modern system that was largely absent or ineffective in the Precambrian and changed in an irreversible manner sometime during the Neoproterozoic. The modern ocean buries 1.6×10^{14} g C/year, of which 86% (1.38×10^{14} g C/year) is buried in ocean margins (*11*), where OC concentration and hence burial flux is linearly proportional to clay content. Applying this burial rate throughout the Phanerozoic and assuming that the peak ratios in Fig. 2 are proportional to clay content, then the clay-driven increase in OC burial that developed during 730 to 500 Ma (Fig. 2) ramped from 0.21×10^{14} to 1.38×10^{14} g C/year. The resulting sixfold increase in oxygen retention would have greatly influenced biogeochemical cycling of redox sensitive elements such as Fe^{+2} and S^{2-} (*2*, *3*, *5*) and ultimately increased the oxygen concentration of the atmosphere. The evolutionary innovation and expansion of land biota could permanently increase weathering intensity and PCM formation, establishing a new level of organic carbon burial and oxygen accumulation.

References and Notes

1. L. A. Derry, A. J. Kaufman, S. B. Jacobsen, *Geochim. Cosmochim. Acta* **56**, 1317 (1992).
2. L. C. Kah, T. W. Lyons, T. D. Frank, *Nature* **431**, 834 (2004).
3. D. E. Canfield, A. Teske, *Nature* **382**, 127 (1996).
4. D. J. Des Marais, H. Strauss, R. E. Summons, J. M. Hayes, *Nature* **359**, 605 (1992).
5. S. T. Brennan, T. K. Lowenstein, J. Horita, *Geology* **32**, 473 (2004).
6. P. Cloud, *Paleobiology* **2**, 351 (1976).
7. B. Runnegar, *Alcheringa* **6**, 223 (1982).
8. A. H. Knoll, *Life on a Young Planet* (Princeton Univ. Press, Princeton, NJ, 2003), p. 247.
9. J. Brocks, G. A. Logan, R. Buick, R. E. Summons, *Science* **285**, 1033 (1999).
10. R. G. Keil, E. Tsamakis, C. B. Fuh, J. C. Giddings, J. I. Hedges, *Geochim. Cosmochim. Acta* **58**, 879 (1994).
11. J. I. Hedges, R. G. Keil, *Mar. Chem.* **49**, 81 (1995).
12. L. M. Mayer, L. L. Schick, K. R. Hardy, R. Wagai, J. McCarthy, *Geochim. Cosmochim. Acta* **68**, 3863 (2004).
13. L. M. Mayer, *Geochim. Cosmochim. Acta* **58**, 1271 (1994).
14. B. Ransom, K. Dongseon, M. Kastner, S. Wainwright, *Geochim. Cosmochim. Acta* **62**, 1329 (1998).
15. R. G. Keil, D. B. Montlucon, F. G. Prahl, J. I. Hedges, *Nature* **370**, 549 (1994).
16. M. J. Kennedy, D. R. Pevear, R. J. Hill, *Science* **295**, 657 (2002).
17. R. Cox, D. R. Lowe, R. L. Cullers, *Geochim. Cosmochim. Acta* **59**, 2919 (1995).
18. R. M. Garrels, F. T. Mackenzie, *Evolution of Sedimentary Rocks* (Norton, New York, 1971), p. 397.
19. C. E. Weaver, *Clays, Muds and Shales* (Developments in Sedimentology, Elsevier, New York, 1989), p. 819.
20. A. B. Ronov, *Geokhimiya* **8**, 715 (1964).
21. R. H. Dott Jr., *J. Geol.* **111**, 387 (2003).
22. W. V. Preiss, *Bull. Geol. Surv. S. Australia* **53**, 438 (1987).
23. The Schultz ratio is an uncalibrated, dimensionless number that specifically indicates the relative amount of total phyllosilicates versus quartz by using the x-ray peak intensities for the sum of all phyllosilicates (020 peak, 19.8° 2 Θ, Cu Ka radiation) and quartz (100 peak, 20.8° 2Θ) on random powder mounts. For a granite or clean sandstone, this number would be <0.2. For mudstones and pelitic metamorphics (clay shales, mudstones, slates, and mica schists), it typically is between 0.2 and 2.0. Sediment derived from fine grinding of granite to clay size does not change the Schultz ratio unless dissolution and reprecipitation as a clay mineral has occurred. It is an indicator of available clay minerals in the provenance area, both recycled, and newly formed by soil processes. Later clay diagenesis (such as illitization) does not change the Schultz ratio because it typically converts one phyllosilicate to another.
24. H. Chamley, *Clay Sedimentology* (Springer, Berlin, 1989), p. 623.
25. L. G. Schultz, *U. S. Geol. Surv. Tech. Rep. No. 391C* (1964).
26. G. Shields, J. Veizer, *Geochem. Geophys. Geosystems* **3**, 1 (2002).
27. G. J. Retallack, *Soils of the Past, an Introduction to Pedology* (Blackwell Science, Oxford, ed. second, 2001), p. 404.
28. A. R. Prave, *Geology* **30**, 811 (2002).
29. R. J. Horodyski, L. P. Knauth, *Science* **263**, 494 (1994).
30. D. S. Heckman *et al.*, *Science* **293**, 1129 (2001).
31. X. Yuan, S. Xiao, T. N. Taylor, *Science* **308**, 1017 (2005).
32. A. Neaman, J. Chorover, S. L. Brantley, *Am. J. Sci.* **305**, 147 (2005).
33. S. E. Campbell, *Origins Life* **9**, 335 (1979).
34. J. F. Banfield, W. W. Barker, S. A. Welch, A. Taunton, J. V. Smith, *Proc. Natl. Acad. Sci. U.S.A.* **96**, 3404 (1999).
35. J. A. Raven, D. Edwards, *J. Exp. Bot.* **52**, 381 (2001).
36. C. France-Lanord, L. A. Derry, *Nature* **390**, 65 (1997).
37. A. H. Knoll, S. B. Carroll, *Science* **284**, 2129 (1999).
38. F. L. Lynch, *Clays Clay Miner.* **45**, 618 (1997).

39. We thank S. Jensen, T. Bristow, G. Jiang, J. Gehling, and M. Fuller for help in the field. This work was sponsored by NASA grant NWG04GJ42G and NSF-EAR grants 0223198 and 0345207.

Supporting Online Material
www.sciencemag.org/cgi/content/full/1118929/DC1
Materials and Methods
Table S1
References and Notes

16 August 2005; accepted 13 December 2005
Published online 2 February 2006;
10.1126/science.1118929
Include this information when citing this paper.

The Last Deglaciation of the Southeastern Sector of the Scandinavian Ice Sheet

V. R. Rinterknecht,[1*†] P. U. Clark,[1] G. M. Raisbeck,[2] F. Yiou,[2] A. Bitinas,[3] E. J. Brook,[1] L. Marks,[4] V. Zelčs,[5] J.-P. Lunkka,[6] I. E. Pavlovskaya,[7] J. A. Piotrowski,[8] A. Raukas[9]

The Scandinavian Ice Sheet (SIS) was an important component of the global ice sheet system during the last glaciation, but the timing of its growth to or retreat from its maximum extent remains poorly known. We used 115 cosmogenic beryllium-10 ages and 70 radiocarbon ages to constrain the timing of three substantial ice-margin fluctuations of the SIS between 25,000 and 12,000 years before the present. The age of initial deglaciation indicates that the SIS may have contributed to an abrupt rise in global sea level. Subsequent ice-margin fluctuations identify opposite mass-balance responses to North Atlantic climate change, indicating differing ice-sheet sensitivities to mean climate state.

At its maximum extent, the Scandinavian Ice Sheet (SIS) merged with the Barents Ice Sheet (BIS) and Kara Ice Sheet to form a Eurasian ice sheet complex that was the second largest of the former Northern Hemisphere ice sheets (*1*–*3*). Such a large ice mass would have influenced climate on scales ranging from regional to hemispheric and may have affected the formation of North Atlantic deepwater through releases of meltwater and icebergs. Simulations with climate models suggest that the mass balance of the SIS was particularly sensitive to changes in North Atlantic climate because of its location immediately downwind of the North Atlantic Ocean (*4*). Finally, the SIS deformed the underlying crust, and the record of postglacial isostatic recovery can be inverted to reveal geophysical properties of the lithosphere and mantle (*5*, *6*).

Isolating the relative contributions of the SIS to changes in global sea level, climate, and the solid Earth requires that the chronology of its growth and decay be well constrained. Ice-

[1]Department of Geosciences, Oregon State University, Corvallis, OR 97331, USA. [2]Centre de Spectrométrie Nucléaire et de Spectrométrie de Masse, 91405 Orsay, France. [3]Geological Survey of Lithuania, LT-03123 Vilnius, Lithuania. [4]Polish Geological Institute, 00-975 Warsaw, Poland. [5]Department of Geography and Earth Sciences, University of Latvia, Riga, LV-1586, Latvia. [6]Institute of Geosciences, University of Oulu, Post Office Box 3000, Linnanmaa 90014, Finland. [7]National Academy of Sciences of Belarus, Institute of Geological Sciences, 220141 Minsk, Belarus. [8]Department of Earth Sciences, University of Aarhus, DK-8000 Aarhus, Denmark. [9]Institute of Geology, Tallinn University of Technology, 10143 Tallinn, Estonia.

*Present address: Lamont-Doherty Earth Observatory, Columbia University, Palisades, NY 10964, USA.
†To whom correspondence should be addressed. E-mail: vincent@ldeo.columbia.edu

rafted debris (IRD) in marine cores often provide well-dated records of ice-sheet variability (*7*, *8*), but the linkages between the physics of ice sheets and the formation of an IRD signal have not been clearly established. Prominent end moraines deposited by the southern SIS margin across northern Europe provide a direct record of ice-margin fluctuations, but the paucity of organic material for radiocarbon dating in this region has prevented the development of more than a general understanding of the timing of these fluctuations (*9*). We measured cosmogenic ^{10}Be concentrations in samples associated with six main moraines (*10*) deposited by the southeastern SIS in Poland, Belarus, Lithuania, Latvia, Estonia, and Finland (Fig. 1) that firmly establish the chronology of the southern SIS margin since 25,000 years before the present (25 kyr B.P.).

Boulder exposure ages were calculated from ^{10}Be/^{9}Be ratios measured by accelerator mass spectrometry (table S1) (*10*). We present the moraine age as either the mean exposure ^{10}Be age or the error-weighted mean exposure ^{10}Be age, and the uncertainty as the larger of the standard deviation of the mean exposure ages or the error-weighted mean of the analytical uncertainty (*10*). Outliers exist in the exposure-age populations of all but one of the SIS moraines (Fig. 2). We attribute the anomalously old ages (generally ≥30 ^{10}Be kyr) to incomplete erosion of boulder surfaces that had previously been exposed to secondary cosmic rays, resulting in ^{10}Be inheritance. Exposure ages that are clearly too young (generally ≤10 ^{10}Be kyr) may reflect post-depositional exhumation or movement or unrecognized erosion of boulder surfaces. Accordingly, we removed these outliers and then further reduced the data set by using Chauvenet's criterion (*11*) to reject outliers from the sample population of a given moraine, reducing our measured data set from 138 to 111 ^{10}Be ages (*10*). We then combined previously published ^{10}Be data on four samples from the Salpausselkä I moraine in Finland (*12*) with data on our nine samples from that moraine (*13*).

By combining our new ^{10}Be data with 70 new and existing limiting radiocarbon ages on interstadial or postglacial organic matter (table S2), we developed a comprehensive chronology of the southeastern margin of the SIS that identifies three ice-margin fluctuations between 25,000 and 12,000 calendar (cal) yr B.P. (Fig. 3A). Calibrated radiocarbon ages indicate that after a long interstadial, the SIS margin advanced into the Baltic lowlands after 24,900 ± 370 cal yr B.P. (*14*) and reached its maximum extent marked by the Last Glacial Maximum (LGM) Moraine after 20,980 ± 270 cal yr B.P. (*15*) (Fig. 3A). We interpret the cosmogenic ages on surface boulders from moraines to represent the final time of moraine formation. Our 10 ^{10}Be ages from the LGM Moraine in Belarus and Lithuania (Fig. 2A) thus suggest that the SIS margin began to retreat from its

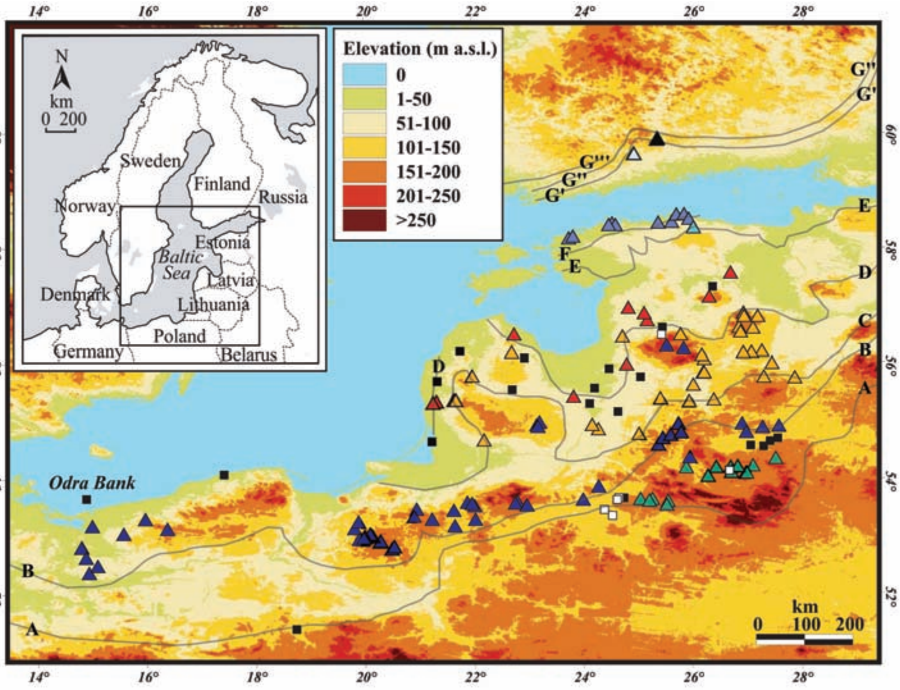

Fig. 1. Digital elevation model of the sampling area (adapted from http://lpdaac.usgs.gov). The main ice-marginal positions are outlined in gray (*21*). a.s.l., above sea level. (**A**) LGM Moraine. (**B**) Pomeranian Moraine. (**C**) Middle Lithuanian Moraine. (**D**) North Lithuanian Moraine. (**E**) Pandivere Moraine. (**F**) Palivere Moraine. (**G′**) Salpausselkä I Moraine. (**G″**) Salpausselkä II Moraine. (**G‴**) Salpausselkä III Moraine. ^{10}Be sites are indicated as follows: LGM Moraine (green-blue triangles), Pomeranian Moraine (dark blue triangles), Middle Lithuanian Moraine (orange triangles), North Lithuanian Moraine (red triangles), Pandivere Moraine (light blue triangle), Palivere Moraine (purple triangles), Salpausselkä I Moraine (gray triangle represents nine samples) (*13*), Salpausselkä I Moraine (black triangle represents four samples) (*12*). ^{14}C sites are indicated as follows: this study (white squares), previous studies (black squares).

maximum limit at 19,000 ± 1600 ^{10}Be years (Fig. 3A).

Radiocarbon ages on peat from the Odra Bank of the Baltic Sea (*16*), 20 km north of the Polish coast (Fig. 1), indicate that the ice margin retreated north of this site before 16,760 ± 360 cal yr B.P., in good agreement with our new radiocarbon age for interstadial sediments in Lithuania (16,470 ± 230 cal yr B.P.; laboratory number AA-53595) (Fig. 3A and table S2). The younger age at Odra Bank indicates that the site remained unglaciated until after 15,520 ± 430 cal yr B.P., when ice subsequently readvanced to the Pomeranian Moraine. A similar age for ice recession (~15,400 cal yr B.P.) had previously been inferred from radiocarbon dating of organic deposits at the Raunis site, Latvia (*15*), which became a key constraint in interpretations of SIS marginal history (*9*). Subsequent investigations, however, demonstrated that these deposits are thoroughly penetrated by recent rootlets (*17*, *18*), pointing to possible radiocarbon contamination.

Forty-two ^{10}Be ages from the Pomeranian Moraine have a mean age of 14,600 ± 300 ^{10}Be years (Fig. 2B), which is significantly younger than the previous moraine-age estimate of ~18,000 cal yr B.P. (*19*–*21*). Combined with the Odra Bank radiocarbon ages, these data identify a significant post-LGM fluctuation of the SIS margin, with readvance from north of the Baltic coast to within 50 to 100 km of the LGM Moraine after ~15,500 cal yr B.P. and a subsequent retreat beginning at ~14,600 ^{10}Be years (Fig. 3A). The ^{10}Be ages from three younger Baltic recessional moraines and one boulder from the Pandivere Moraine indicate a relatively slow retreat of the SIS margin from the Pomeranian Moraine to a position south of the Baltic coast by ~13,000 ^{10}Be years (Figs. 2, C to F, and 3A). With the exception of two radiocarbon ages from Poland [the Gardno site (*23*, *24*)] and two radiocarbon ages from Latvia [the Progress site (*17*, *18*)], our 92 ^{10}Be ages dating ice retreat from the Pomeranian Moraine to the south coast of the Baltic Sea are in excellent agreement with 23 ^{14}C ages on postglacial organic material that provide minimum ages for deglaciation of the same region (Fig. 3A and table S2).

The third and youngest fluctuation of the southern SIS occurred after ice-margin retreat several tens of kilometers north of what is now the Salpausselkä I Moraine before it readvanced to deposit that moraine (Fig. 3A) (*25*). When we combine our ^{10}Be data from the Salpausselkä I Moraine with those of Tschudi *et al*. (*12*) and use an integrated production rate to account for

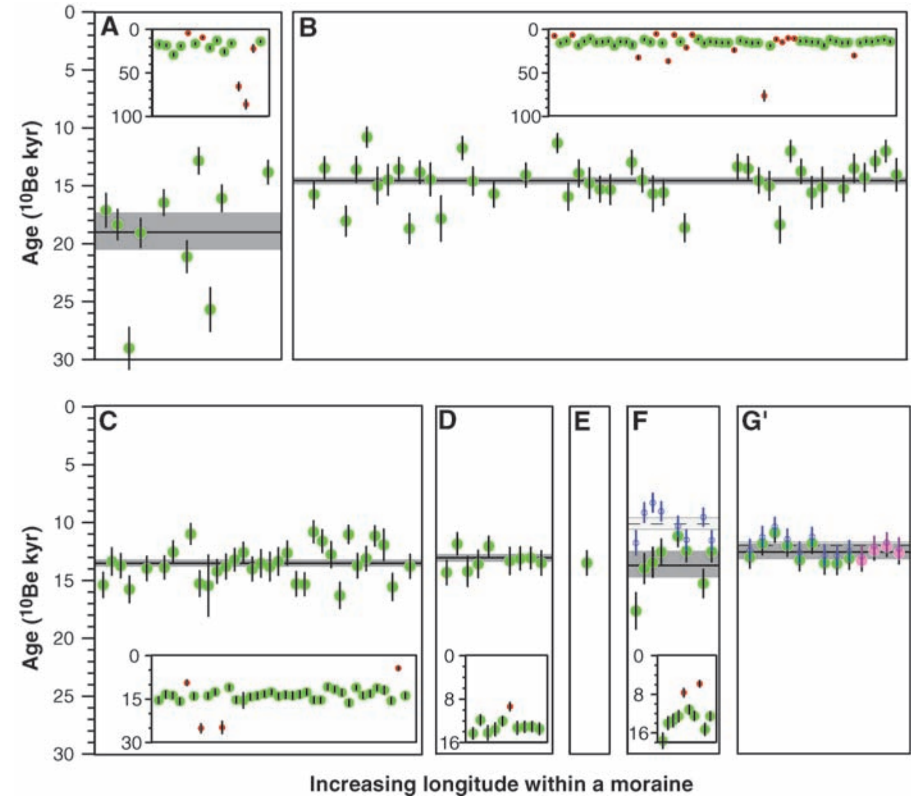

Fig. 2. Single ^{10}Be exposure ages (green and red symbols). (**A**) LGM Moraine [mean age = 19.0 ± 1.6 ^{10}Be thousand years ago (ka), n = 10 samples]. (**B**) Pomeranian Moraine (mean age = 14.6 ± 0.3 ^{10}Be ka, n = 42). (**C**) Middle Lithuanian Moraine (mean age = 13.6 ± 0.3 ^{10}Be ka, n = 32). (**D**) North Lithuanian Moraine (error-weighted mean age = 13.1 ± 0.3 ^{10}Be ka = 9). (**E**) Pandivere Moraine (13.1 ± 1.1 ^{10}Be ka, n = 1). (**F**) Palivere Moraine (mean age = 13.6 ± 1.2 ^{10}Be ka, n = 8). (**G′**) Salpausselkä I Moraine (error-weighted mean age = 12.5 ± 0.7 ^{10}Be ka, n = 13). ^{10}Be exposure ages are ordered within a moraine using the sample longitudes (west to east). Insets in (A) to (D) and (F) correspond to the full data set. Green symbols are ^{10}Be exposure ages used in the moraine age calculation. Red symbols are outliers not included in the moraine age. Error bars for single ^{10}Be exposure ages correspond to 1σ analytical uncertainty only. The black horizontal lines identify the mean age or the error-weighted mean age for each moraine. Shaded gray bands correspond to 1σ uncertainty (the standard deviation of the mean exposure age or error-weighted mean of the analytical uncertainties combined when necessary with uncertainties associated with water submergence and/or uplift assumptions). Pink symbols in (G′) are the ^{10}Be data from Tschudi *et al.* (*12*), recalculated using our corrected production rate and erosion and uplift assumptions (*13*). Open symbols in (F) and (G′) correspond to ^{10}Be samples uncorrected for estimated water submergence and/or isostatic uplift (*10*). The black dashed line corresponds to the moraine mean age in (F) (10.1 ± 0.5 ^{10}Be ka, n = 8), and to the moraine error-weighted mean age in (G′) (12.0 ± 0.2 ^{10}Be ka, n = 13) for these uncorrected ages.

isostatic uplift of the region (*10*), we find that ice retreat from the moraine began at 12,500 ± 700 ^{10}Be years (*13*) (Figs. 2G′ and 3A).

Our new chronology for the southern SIS margin has several important implications for understanding the response of the SIS to climate change and its contribution to global sea level change. Our constraints on the timing of the southern SIS at its last maximum extent (~21 cal kyr B.P. to 19.0 ^{10}Be kyr) are in good agreement with ages constraining a major advance of the western SIS margin (*26*) and the maximum extent of the BIS margin (*27*, *28*). Because the SIS and BIS coalesced at their maximum extent, this agreement indicates the expansion of much of the Eurasian ice sheet complex to its full glacial extent during the interval of relative climate stability and low sea level of the LGM (19.0 to 23.0 kyr B.P.).

Within dating uncertainties, our new ages suggest that the onset of deglaciation of the southern SIS margin at ~19.0 ^{10}Be kyr may be synchronous with a rapid sea-level rise of 10 to 15 m at ~19.0 cal kyr B.P. that abruptly terminated the LGM lowstand (*29*) (Fig. 3B). Clark *et al.* (*30*) inferred that the source of this event originated from one or more of the Northern Hemisphere ice sheets. Our dating of the retreat of the southern SIS margin at this time provides direct evidence that the SIS may have contributed to this abrupt sea-level event. The abruptness of the sea-level event in the absence of any associated abrupt warming (Fig. 3, B and C) points to an instability of the SIS that caused it to partially collapse, although the gradual warming that preceded the event suggests the possibility of a nonlinear response of the ice sheet to that warming (*31*). Such a response may have induced fast flow (*32*) and drawdown of the low-sloping Baltic Sea ice stream (*21*), causing retreat of the southeastern SIS margin.

This phase of early deglaciation was followed by a 3 to 4 kyr interval of restricted SIS margin extent that coincides with a reduction of the Atlantic meridional overturning circulation induced by the 19-kyr sea-level event and subsequent Heinrich event 1 (H1) (Fig. 3D) (*30*, *33*), with the attendant loss of ocean heat transport to the North Atlantic region causing the Oldest Dryas cold interval (Fig. 3C). Why did the southern SIS margin remain retracted during this cold interval? We suggest that the southward expansion of the polar front in the North Atlantic associated with H1 (*34*), with an attendant increase in sea ice coverage, caused moisture starvation of the SIS (*4*), thus preventing its margin from readvancing. Evidence in support of this hydrologic response comes from proxy records that indicate that extreme aridity over Europe accompanied cold temperatures during Heinrich events (*35*).

We attribute the subsequent readvance of the southern SIS margin to the Pomeranian Moraine to the initial warming that occurred in the North Atlantic region after H1 but before the large and abrupt warming marking the onset of the Bølling-Allerød (Fig. 3, A and C). In particular, a more positive SIS mass balance and attendant ice-margin readvance are expected outcomes of such a warming as a consequence of the precipitation-temperature feedback, which is most effective under cold climates (*36*). Pollen records support the idea that this atmospheric hydrologic response occurred in showing a rapid shift from semiarid to temperate taxa over parts of southern Europe starting at ~16 cal kyr B.P. (*35*).

The large-scale recession of the southern SIS margin beginning at 14,600 ± 300 ^{10}Be years, marking the start of the final retreat of the SIS from the Baltic lowlands, appears to represent a response to the abrupt onset of the Bølling-Allerød warm interval at ~14.6 cal kyr B.P. In this case, the warming to near-interglacial temperatures associated with the Bølling-Allerød interval (Fig. 3C) would have overwhelmed the precipitation-temperature feedback and caused a negative mass balance over the ice sheet (*36*). The ages of the three post-Pomeranian moraines (Figs. 1 and 2C, D, and F) suggest that the receding margin must have paused briefly during the Bølling-Allerød warm interval to construct each of them. Although the precise age of these events cannot be resolved by our dating, the most likely explanation for their occurrence is an ice-margin response to the three centennial-

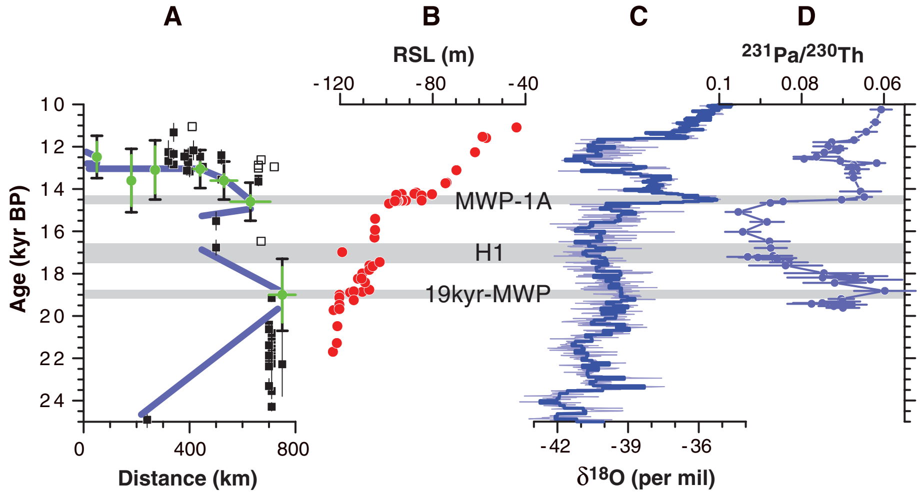

Fig. 3. (**A**) Time-distance diagram showing fluctuations of the southern margin of the SIS as constrained by our mean or error-weighted mean ^{10}Be ages (green circles) (table S1) and calibrated radiocarbon ages (white squares, this study; black squares, previous studies) (table S2). The smallest (green) vertical error bar for each moraine age corresponds to the error as described in (*10*). The largest (black) vertical error bar for each moraine age includes the uncertainty in the ^{10}Be production rate (6%) for comparison with other records. Horizontal uncertainties shown for our ^{10}Be data identify the spatial north-south distance over which samples from each moraine were collected. We calibrated radiocarbon ages younger than 21,381 ^{14}C yr B.P. using IntCal04 (*39*); we calibrated older radiocarbon ages using the Cariaco Basin calibration curve (*40*). We excluded four samples (Gd-6117, Gd-4776, TA-129, and TA-129A; table S2) from this data set because they are probably redeposited or contaminated. (**B**) Records of far-field relative sea-level (RSL) change during the last deglaciation (*29*, *41*, *42*). (**C**) $\delta^{18}O$ record from the Greenland Ice Sheet Project 2 ice core (*43*, *44*). (**D**) Sedimentary $^{231}Pa/^{230}Th$ record from North Atlantic core OCE326-GGC5, a proxy for the Atlantic meridional overturning circulation (*33*).

scale cold events that occurred during the Bølling-Allerød warm interval (Fig. 3C). The short distance (~100 km) separating the Pomeranian and Middle Lithuanian Moraines along the climatically sensitive southern SIS margin is also important in indicating a negligible contribution of the SIS to global sea level rise in response to Bølling-Allerød warming.

Our new ^{10}Be ages confirm the Younger Dryas age of the Salpausselkä I Moraine (*25*) and support the varve chronology (*37*) in showing that the southern SIS margin subsequently began to retreat to the Salpausselkä II Moraine during the Younger Dryas. The presence of the three Younger Dryas moraines may reflect small climate changes during the Younger Dryas affecting SIS mass balance. Alternatively, the small ice-margin retreat may indicate a dynamic response associated with a drawdown of ice through the Gulf of Bothnia. In any event, in contrast to the preceding Pomeranian readvance, which occurred in response to a small warming during a cold climate, the readvance to the Salpausselkä I Moraine occurred in response to a large Younger Dryas cooling during a warm climate. We attribute these opposite responses to the importance of the precipitation-temperature feedback in controlling mass balance only during cold climates (*36*). Similar opposing mass balance changes are projected for the two remaining ice sheets in response to future global warming, with a negative mass balance simulated for the warm-climate Greenland Ice Sheet and a positive mass balance simulated for the cold-climate Antarctic Ice Sheet (*38*).

References and Notes

1. G. H. Denton, T. J. Hughes, *The Last Great Ice Sheets* (Wiley, New York, 1981).
2. P. U. Clark, A. C. Mix, *Quat. Sci. Rev.* **21**, 1 (2002).
3. J. I. Svendsen *et al.*, *Quat. Sci. Rev.* **23**, 1229 (2004).
4. S. W. Hostetler, P. U. Clark, P. J. Bartlein, A. C. Mix, N. J. Pisias, *J. Geophys. Res.* **104**, 3947 (1999).
5. K. Lambeck, C. Smither, P. Johnston, *Geophys. J. Int.* **134**, 102 (1998).
6. G. A. Milne *et al.*, *Science* **291**, 2381 (2001).
7. G. C. Bond, R. Lotti, *Science* **267**, 1005 (1995).
8. K. H. Baumann *et al.*, *Quat. Res.* **43**, 185 (1995).
9. J. Ehlers, P. L. Gibbard, in *Quaternary Glaciations—Extent and Chronology, Part I: Europe*, (Elsevier, Amsterdam, Netherlands, 2004).
10. Materials and methods are available as supporting material on *Science* Online.
11. J. R. Taylor, *An Introduction to Error Analysis*, (University Science Books, Sausalito, CA, 1997).
12. S. Tschudi, S. Ivy-Ochs, C. Schlüchter, P. W. Kubik, H. Rainio, *Boreas* **29**, 287 (2000).
13. V. R. Rinterknecht *et al.*, *Quat. Sci. Rev.* **23**, 2283 (2004).
14. A. Liiva, E. Ilves, J. M. Punning, *Radiocarbon* **8**, 430 (1966).
15. A. A. Velichko, M. A. Faustova, *Quat. Sci. Rev.* **5**, 447 (1986).
16. R. Kramarska, *Geol. Quart.* **42**, 277 (1998).
17. A. Dreimanis, V. Zelčs, in *Glacial Deposits in North-East Europe*, J. Ehlers, S. Kozarski, P. Gibbard, Eds. (A. A. Balkema, Rotterdam, Netherlands, 1995), pp. 105–113.
18. Previous work inferred that a till representing ice readvance overlies organic beds at the Raunis, Latvia, site (*15*). Dreimanis and Zelčs (*17*), however, question the evidence for ice readvance, the stratigraphic context of the dated unit, and the reliability of the radiocarbon dates. Further work on this site and others (the Progress site) is required to confirm their stratigraphic and geochronologic integrity.
19. J. Ehlers, L. Eissmann, L. Lippstreu, H.-J. Stephan, S. Wansa, in (*9*), pp. 135–146.
20. Our mean ^{10}Be age for the Pomeranian Moraine in eastern Europe requires a revision to the longstanding correlation, by way of northern Germany, with the SIS margin in Denmark (*19*, *21*). However, our age is in excellent agreement with the well-dated timing of retreat from the western Swedish coast (*22*).
21. G. S. Boulton, P. Dongelmans, M. Punkari, M. Broadgate, in (*9*), pp. 441–460.
22. J. Lundqvist, B. Wohlfarth, *Quat. Sci. Rev.* **20**, 1127 (2001).
23. K. Rotnicki, R. K. Borkowka, *Prace Państwowego Instytutu Geologicznego* **149**, 84 (1995).
24. The two dated samples (*23*), recovered from cores, are on "organic intercalations" in glacial lake clay and "organogenic infillings" in alluvial fan sediments. In the absence of further details on the dated material, we speculate that these dates may conflict with the age of deglaciation suggested by our ^{10}Be ages as well as the majority of other radiocarbon ages from the Baltic lowlands (table S2) because of contamination. However, these ages are similar to those from the Odra Bank (*16*) and our new radiocarbon age from Lithuania (AA-53595) (table S2) that date an interval of ice retreat, suggesting that the dated material may be reworked organic matter deposited during this interstadial event.
25. H. Rainio, in *Glacial Deposits in North-East Europe*, J. Ehlers, S. Kozarski, P. Gibbard, Eds. (A. A. Balkema, Rotterdam, Netherlands, 1995), pp. 57–66.
26. J. Mangerud, in (*9*), pp. 271–294.
27. J. Y. Landvik *et al.*, *Quat. Sci. Rev.* **17**, 43 (1998).
28. E. Larsen *et al.*, *Boreas* **28**, 115 (1999).
29. Y. Yokoyama, K. Lambeck, P. De Deckker, P. Johnston, L. K. Fifield, *Nature* **406**, 713 (2000).
30. P. U. Clark, A. M. McCabe, A. C. Mix, A. J. Weaver, *Science* **304**, 1141 (2004).
31. H. J. Zwally *et al.*, *Science* **297**, 218 (2002).
32. J. A. Piotrowski, J. Kraus, *J. Glaciol.* **43**, 495 (1997).
33. J. F. McManus, R. Francois, J. M. Gherardi, L. D. Keigwin, S. Brown-Leger, *Nature* **428**, 834 (2004).
34. E. Bard, F. Rostek, J.-L. Turon, S. Gendreau, *Science* **289**, 1321 (2000).
35. N. Combourieu Nebout *et al.*, *Geology* **30**, 863 (2002).
36. H. Le-Treut, M. Ghil, *J. Geophys. Res.* **88**, 5167 (1983).
37. M. Saarnisto, T. Saarinen, *Global Planet. Change* **31**, 387 (2001).
38. P. Huybrechts, J. Gregory, I. Janssens, M. Wild, *Global Planet. Change* **42**, 83 (2004).
39. P. J. Reimer *et al.*, *Radiocarbon* **46**, 1029 (2004).
40. K. Hughen *et al.*, *Science* **303**, 202 (2004).
41. E. Bard, B. Hamelin, R. G. Fairbanks, A. Zindler, *Nature* **345**, 405 (1990).
42. T. K. S. Hanebuth, P. M. Grootes, *Science* **288**, 1033 (2000).
43. P. M. Grootes, M. Stuiver, J. W. C. White, S. Johnsen, J. Jouzel, *Nature* **366**, 552 (1993).
44. M. Stuiver, P. M. Grootes, *Quat. Res.* **53**, 277 (2000).

45. This work was supported by the NSF Paleoclimate Program (E.J.B. and P.U.C.) and the French Institut National de Physique Nucléaire et de Physique de Particules and Institut National des Sciences de l'Univers. We thank S. Tschudi for providing data from the Salpausselkä I Moraine and S. Hostetler, J. Licciardi, J. Mangerud, and anonymous reviewers for comments.

Supporting Online Material

www.sciencemag.org/cgi/content/full/311/5766/1449/DC1
Materials and Methods
Tables S1 and S2
References

28 September 2005; accepted 9 February 2006
10.1126/science.1120702